

Recycling probability and dynamical properties of germinal center reactions

Michael Meyer-Hermann¹, Andreas Deutsch² and Michal Or-Guil²

¹Institut für Theoretische Physik, TU Dresden, D-01062 Dresden, Germany
E-Mail: meyer-hermann@physik.tu-dresden.de

²Max-Planck-Institut für Physik komplexer Systeme,
Nöthnitzer Str.38, D-01187 Dresden, Germany

Abstract: We introduce a new model for the dynamics of centroblasts and centrocytes in a germinal center. The model reduces the germinal center reaction to the elements considered as essential and embeds proliferation of centroblasts, point mutations of the corresponding antibody types represented in a shape space, differentiation to centrocytes, selection with respect to initial antigens, differentiation of positively selected centrocytes to plasma or memory cells and recycling of centrocytes to centroblasts. We use exclusively parameters with a direct biological interpretation such that, once determined by experimental data, the model gains predictive power. Based on the experiment of Han et al. (1995b) we predict that a high rate of recycling of centrocytes to centroblasts is necessary for the germinal center reaction to work reliably. Furthermore, we find a delayed start of the production of plasma and memory cells with respect to the start of point mutations, which turns out to be necessary for the optimization process during the germinal center reaction. The dependence of the germinal center reaction on the recycling probability is analyzed.

1 Introduction

Germinal centers (GCs) are essential elements of the humoral immune response (for a review see MacLennan, 1994). In a primary immunization some B-cells respond to the presented antigen and are activated. These active cells migrate to follicular dendritic cells (FDCs) present in lymphoid tissues. Unprocessed fragments of the antigen, so called epitopes, are expressed on the FDCs. In the milieu of the FDCs the B-cells are in a phase of intense proliferation and show the essential features of B-blasts such that they are denoted as centroblasts. These proliferating centroblasts together with the FDCs develop to a GC.

This morphological development is initiated through an unidentified differentiation signal after about three days. The resulting GC is characterized by two zones (Nossal, 1991): the dark zone filled with continuously proliferating and mutating centroblasts and the light zone containing the FDCs and centrocytes. The latter are generated from the centroblasts (Liu et al., 1991), which are available in great diversity (Weigert et al., 1970) because of a very high mutation rate (Nossal, 1991; Berek & Milstein, 1987). In contrast to centroblasts the centrocytes express antibodies of cell specific types on their surface. In this way they are able to undergo a specific selection process through the interaction with the epitopes presented on the FDCs in the light zone. The diversity of the proliferating and mutating centroblasts together with the specificity of the selection process in the light zone allow an optimization of the affinity between the antibodies and the epitopes. This affinity maturation in the GC leads to a dominant population of cells with high affinity of the corresponding antibodies to the epitopes within 7-8 days after immunization (Jacob et al., 1993).

Centrocytes undergo apoptosis if they are not positively selected in an appropriate range of time. They are rescued from apoptosis (Liu et al., 1989; Lindhout et al., 1993; Lindhout et al., 1995; Choe & Choi, 1998) if they are able to bind to the antigen on the FDCs *and* to interact successfully with T-helper cells present in the external region of the light zone. Even antigen independent signals may be required for the centrocytes to survive (Fischer et al., 1998). Successfully selected centrocytes receive a differentiation signal which determines their fate. They may differentiate into memory cells that are important in the case of a second immunization. Alternatively, they differentiate to antibody producing plasma cells. These are intensifying the immune response in two ways: the number of antibodies increases and their specificity with respect to the direct unspecific immune response without GC reaction is optimized. In both cases the corresponding cell is leaving the GC environment.

A third possibility exists for the positively selected centrocytes: they may be recycled to centroblasts and reenter the highly proliferating and mutating stage of development in the dark zone (Kepler & Perelson, 1993). This recycling hypothesis has been neither directly checked experimentally (for an indirect check see Han et al., 1995b) nor – if true – the probability of recycling is known. It would be of great interest to know about the necessity of a centrocyte recycling process for the affinity maturation. The most evident argument to support the recycling hypothesis is based on the occurrence of multi-step somatic hypermutations in the GC reaction. Under the assumption of random hypermutations, recycling of already mutated cells to fast proliferating centroblasts appears to be a necessary process.

In this paper we estimate how large the recycling probability should be, i.e. which proportion of the positively selected centrocytes should be recycled to get a reliable GC reaction. For this purpose we introduce a simplified model of the GC dynamics based on a functional view on it. The model differs from others (Oprea & Perelson, 1996; Oprea & Perelson, 1997; Rundell et al., 1998) by omitting some details of the GC reaction which we consider as unnecessary to understand the obligatory occurrence of the recycling procedure. On the other hand compared to the model introduced in (Kesmir & de Boer, 1999) we added a formalism to treat somatic hypermutation in a shape space, which seems to be essential to understand the process of affinity maturation. A very important difference to related models is that we embed the experiment (Han et al., 1995b) for the first time. This experiment provides an indirect evidence for the existence of the recycling process and we will interpret it in a quantitative way in order to extract information on the recycling probability from it. We use exclusively parameters with a direct biological interpretation to ensure the predictive power of the model.

In the next section we will define the shape space, in which the cell population dynamics takes place, and the corresponding dynamical quantities and parameters including their dynamical interdependence. All parameters introduced in the model are determined by experimental observations. The third section is dedicated to the presentation and interpretation of the model in comparison with experimental GC reactions. We will analyze the stability of our results to verify the notion of a prediction. Finally, we investigate the dependence of some characteristics of the germinal center reaction on the variation of the recycling probability and give some concluding remarks.

2 Definition of the model

2.1 Shape space and affinity space

Postulates Before defining a model for the GC dynamics it is necessary to specify the space in which the dynamics takes place. As we want to represent cells corresponding to different types of antibodies we use the well known shape space concept (Perelson & Oster, 1979). This ansatz is based on the following assumptions:

- Antibodies can be represented in a phenotypical shape space.
- Mutation can be represented in the shape space by next-neighbor jumps.
- Complementarity of antibodies and antigen.
- Homogeneity of the affinity weight function on the shape space.

Representation of antibody phenotype The shape space is taken as a D -dimensional finite size lattice of discrete equidistant points, each of them representing one specific antibody type. Thus the shape space becomes a phenotype space, i.e. it is not primarily a representation of genetic codes but of the resulting features due to specific genetic codes.

Representation of mutation Nevertheless, we want to represent point mutations defined in an unknown genotype space in the shape space. To this end we are compelled to formulate the action of a point mutation in the shape space:

A point mutation of a given antibody is represented in the phenotypical shape space by a jump to one of the nearest neighbor points.

This assumption is not very spectacular as it only requires that a point mutation does not lead to a random jump of the antibody phenotype, i.e. that conformation, electrical properties, etc. are not dramatically changed. Surely, the mutation of some key base pairs may exist which imply fundamental changes of the encoded antibody features. However, these exceptions will not alter the dynamics of the GC until the number of such key base pairs remains small with respect to the number of *smooth* mutation points.

Antigen representation and complementarity A central quantity is the affinity of a given antibody and an antigen epitope. Having a representation of antibodies in the shape space, a counterpart for antigens is necessary. We emphasize that the number of possible antibodies is finite, whereas the diversity of antigens is principally unbounded. Therefore, we represent an antigen on the B-cell shape space at the position of the B-cell with highest affinity to the antigen, i.e. at the position of an antibody with optimal complementarity to the antigen.

Property of smooth affinity Starting from these assumptions (phenotype shape space, representation of mutation by next-neighbor jumps, and complementarity) we have reached a representation of antibodies and antigens in a shape space, which has the property of *affinity neighborhood*, i.e. that neighbor points in the shape space have comparable affinity to a given antigen. This property is a direct consequence of the definition of mutations in a (phenotype) shape space. Starting from a non-directed mutation as base for affinity maturation in GCs, we estimate the affinity neighborhood as a necessary property of the underlying shape space. An initial B-cell with a particular affinity to a certain antigen must have the possibility of successively optimizing the affinity, i.e. of stepwise climbing an *affinity hill*. If no affinity neighborhood would exist, i.e. if there was a random affinity distribution on the shape space, each mutation would lead to a random jump in the affinity. An optimization of the affinity to the antigen may occur accidentally in this scenario, but should be a very rare event.

Homogeneous affinity weight function Affinity neighborhood allows for the definition of an *affinity weight function* which determines the affinity of antigen and antibody in dependence of their distance in the shape space. We assume this weight function $a(\phi, \phi^*)$ to apply equally well in all regions of the shape space which corresponds to a homogeneous affinity distribution over the shape space, and to be of exponential form:

$$a(\phi, \phi^*) = \exp\left(-\frac{\|\phi - \phi^*\|^\eta}{\Gamma^\eta}\right) \quad (1)$$

where Γ is the width of the affinity weight function and $\|\cdot\|$ denotes the Euclidean metric. The question remains with which exponent η the distance enters the exponential weight

function and it will be argued that $\eta = 2$ is a reasonable value (see Fig. 2).

2.2 Formulation of the dynamics

Having a shape space at hand it is possible to define distributions $B(\phi)$, $C(\phi)$, $A(\phi)$, and $O(\phi)$ of centroblasts, of centrocytes, of the presented antigen epitopes, and of the plasma and memory cells on the shape space (see Tab. 1). We focus on the centroblast distribution B and analyze its dynamical behavior in the different phases of the GC reaction.

Cell type	Variable	Processes
antigen	$A(\phi)$	interaction with centrocytes
centroblasts	$B(\phi)$	proliferation mutation differentiation to centrocytes
centrocytes	$C(\phi)$	selection and apoptosis recycling to centroblasts
plasma and memory cells	$O(\phi)$	differentiation to plasma and memory cells removed from GC

Table 1: The variables in the mathematical model of the GC reaction and the processes that are considered.

There were several attempts to divide the germinal center reaction in different working phases. From the point of view of our model we are led to a new functional phase distinction of the GC reaction (see Fig.1). Our three-phase description of the GC reaction is in accordance with most of the models established so far (see e.g. MacLennan, 1994; Liu et al., 1991; Kelsoe, 1996) but is in contradiction to the time scales found in (Camacho et al., 1998), which differ strongly. It is not intended to find mechanisms of transition between the phases of the germinal center reaction. These dynamical phases are assumed according to experimental observations.

The first phase is the already mentioned phase of fast proliferation of a low number of seeder cells in the environment of FDCs. In this phase it is likely that somatic hypermutation is not taking place to a relevant amount (Han et al., 1995b; Jacob et al., 1993; McHeyzer-Williams et al., 1993; Pascual et al., 1994b) such that it may be understood as an enlargement phase of the cell pool available for the following process of affinity maturation. The corresponding dynamical behavior of the centroblast distribution is described as

$$\frac{dB}{dt}(\phi) = pB(\phi) \quad \text{for } t - t_0 < \Delta t_1 \quad , \quad (2)$$

where p denotes the proliferation rate and t_0 is the time of first immunization. This phase lasts $\Delta t_1 = 3$ days and is well established by experiment (Liu et al., 1991).

After three days the optimization phase starts. The GC gets its morphological form, i.e. dark and light zones emerge. In the dark zone centroblasts continue to proliferate but, additionally, somatic hypermutations are broadening the initial centroblast distribution on the shape space. At the same time the selection process operates in the light zone and

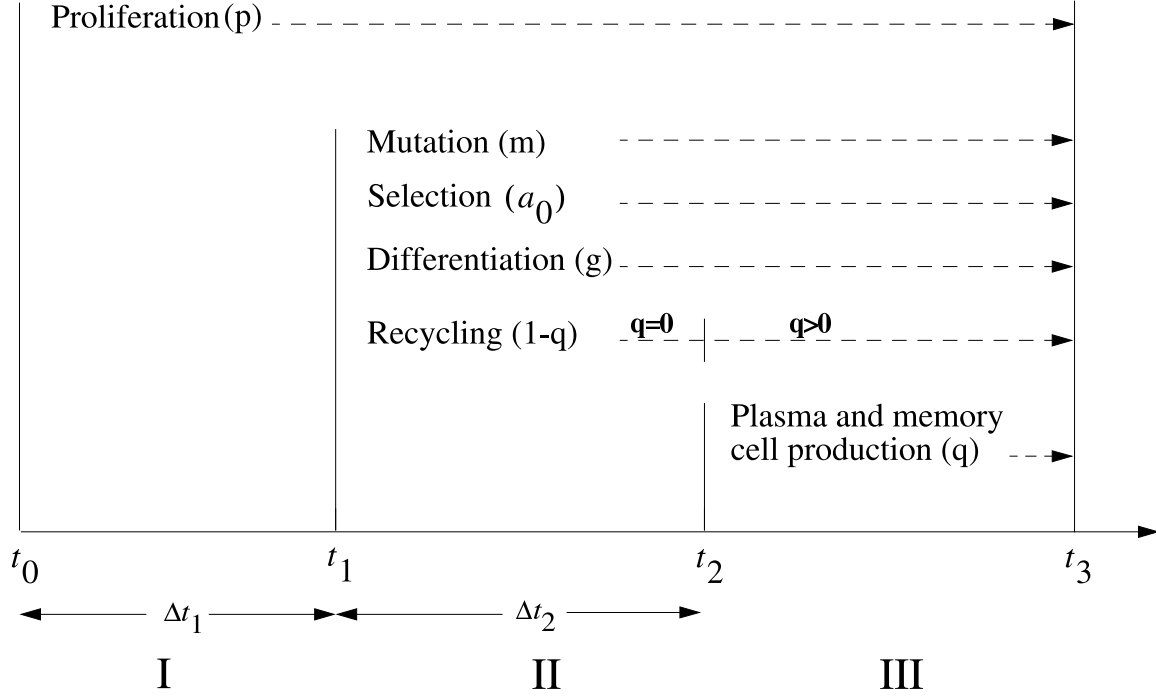


Figure 1: The three model phases of the germinal center reaction: (I) proliferation phase (starting at $t_0 = -3d$), (II) optimization phase (starting at $t_1 = 0d$, the duration Δt_2 is determined in Sec. 2.8), (III) output phase (ending at $t_3 = 18d$). The parameters in brackets refer to the model equations Eq. (2), Eq. (3), Eq. (6), and Eq. (8) and can be determined from experimental data (see Sec. 2.2-2.8).

the selected centrocytes are either recycled to centroblasts or differentiate to plasma and memory cells. The development of the centroblast distribution on the shape space is now described by

$$\begin{aligned} \frac{dB}{dt}(\phi) = & (p - 2pm - g)B(\phi) + \frac{pm}{D} \sum_{\|\Delta\phi\|=1} B(\phi + \Delta\phi) \\ & + (1 - q) \sum_{\phi^*} C(\phi)A(\phi^*) a_0 a(\phi, \phi^*) \quad , \end{aligned} \quad (3)$$

for $t - t_0 \geq \Delta t_1$. Here, g is the rate of centroblast differentiation into centrocytes. m is the mutation probability, a_0 is the probability of an optimal centrocyte to be positively selected, q is the probability of differentiation into plasma and memory cells for positively selected centrocytes, and D is the dimension of the underlying shape space. The different contributions to Eq. (3) are discussed in detail below. Note that this equation does not include eventual finite size effects due to small populations.

It is not clear a priori, if differentiation into antibody producing plasma and memory cells is triggered already in this second phase. To allow a start of the output cell production delayed by the time interval Δt_2 we divide the optimization phase into two sub-phases

which differ in the output probability q :

$$\begin{aligned} q &= 0 & \text{for } 0 \leq t - \Delta t_1 < \Delta t_2 \\ q &> 0 & \text{for } 0 \leq t - \Delta t_2 < \Delta t_3 \quad . \end{aligned} \quad (4)$$

The time delay Δt_2 will be fixed by experimental data (see Sec. 2.8). The output phase include optimization and production of plasma and memory cells and lasts for the remaining GC life-time, which is about $\Delta t_3 = 21\text{days} - 3\text{days} - \Delta t_2$ (Choe & Choi, 1998; Kelsoe, 1996; Jacob et al., 1991). Then, only a few proliferating B-blasts remain in the environment of the FDCs (Liu et al., 1991).

Proliferation

During the whole GC reaction a fast proliferation of B-cells takes place. After the activation of B-cells by an interaction with an antigen, these move to FDCs and undergo a fast proliferation phase in their environment (Liu et al., 1991; Hanna, 1964; Zhang et al., 1988; Grouard et al., 1995). It is likely that the fast proliferation is triggered by the dendritic cells (Dubois et al., 1999). After about three days (Liu et al., 1991) when the GC starts to develop its characteristic light and dark zone (Camacho et al., 1998), a fast proliferation of centroblasts is still observed in the dark zone. The extremely high rate of proliferation could be determined to be (Liu et al., 1991; Zhang et al., 1988)

$$\frac{p}{\ln(2)} \approx \frac{1}{6h} \quad , \quad (5)$$

a result known already for a long time (Hanna, 1964). The population of centroblasts at ϕ grows exponentially, which is represented by the term $pB(\phi)$ in Eq. (2) and Eq. (3).

Mutation

It is likely that somatic hypermutation does not occur in the proliferation phase of the GC reaction (Han et al., 1995b; Jacob et al., 1993; McHeyzer-Williams et al., 1993; Pascual et al., 1994b). On the other hand the growth of the centroblast population is reduced by possible mutations from state ϕ to its neighbors $\phi + \Delta\phi$, where $||\Delta\phi|| = 1$. In a continuous space this corresponds to a diffusion process as used in (Perelson & Wiegel, 1999) to represent mutation. Each pair of cells produced by proliferation will populate a neighbor state with a probability of m . This mutation probability turns out to take extremely high values of $m \approx 1/2$ (Nossal, 1991; Berek & Milstein, 1987), which corresponds to a factor 10^7 larger probability compared to mutations outside the GCs (Janeway & Travers, 1997). We want to point out that here only point mutations of phenotypical relevance are taken into account. As a consequence the population growth by proliferation is reduced by the important amount $2pm$, which results in an effective proliferation rate at ϕ of $p(1 - 2m)$. One observes that for $m = 1/2$ the two first terms in Eq. (3) cancel. This corresponds to the situation that in each centroblast replication one new cell remains in the old state and the second new cell mutates to a neighbor state such that the total number of cells in state ϕ remains unaltered.

In the same way as mutation depopulates the state ϕ in the shape space and populates its neighbors, ϕ is populated by its neighbors. This gives rise to the non-diagonal term in Eq. (3). Each neighbor of ϕ mutates with the same rate $2pm$ from $\phi + \Delta\phi$ to one of its $2D$ neighbors. Only the mutation from $\phi + \Delta\phi$ to the particular neighbor ϕ enhances the population of centroblasts at ϕ such that the rate is weighted by the inverse number of neighbors $1/(2D)$ and is summed over all possible neighbors of ϕ .

Selection, recycling and cell production

After the establishment of the light and dark zones in the GC the differentiation of centroblasts to antibody presenting centrocytes is triggered to allow a selection process in the light zone. The centroblasts in the shape space state ϕ are diminished with the rate of differentiation g , leading to the term $-gB(\phi)$ in Eq. (3). The centrocyte population $C(\phi)$ of type ϕ is enhanced simultaneously by the same amount of cells:

$$C(\phi) = +gB(\phi) \quad . \quad (6)$$

The centrocytes move to the light zone where they undergo a selection process. Their further development is splitted three-fold. The non-selected centrocytes die through apoptosis and are eliminated from the GC dynamics. It is known for a long time that the centrocytes undergoing apoptosis were in cell cycle a few hours ago (Fliedner, 1967) such that it is likely that they differentiated from the centroblasts. On the other hand apoptosis takes place in the light zone (Hardie et al., 1993) where centroblasts are not present in high density. The selected centrocytes are emitted from the GC with probability q and differentiate either into antibody producing plasma cells or to memory cells. The model does not distinguish between plasma and memory cells. Only their sum is taken into account and is denoted by *output cells* $O(\phi)$. Nevertheless, the dynamics of both types of output cells may be different (Choe & Choi, 1998). Also, the degree of affinity maturation differs (Smith et al., 1997). In addition, we do not consider any further proliferation of output cells in or outside of the GC, which may be important for a quantitative comparison with experimental measurements.

Alternatively the selected centrocytes are recycled to become centroblasts and to reenter the proliferation process in the dark zone. This happens with probability $1 - q$ and contributes to the centroblast distribution, corresponding to the last term in Eq. (3).

We want to emphasize that we do not resolve the time course of the selection process, which is regarded to be fast with respect to the centroblast proliferation time scale. This procedure is justified by a minimal duration of a typical selection process of 1 – 2 hours (van Eijk & de Groot, 1999), which is about one fourth of the proliferation time scale. Nevertheless, one should be aware of possible implications due to the fact that the selection process does not occur instantaneously. We effectively enclose the selection time in the parameter g , which in this way becomes a measure of a complete selection cycle including the differentiation into centrocytes, a first selection at the FDCs, a second selection at T-helper cells and finally the recycling process. This has two consequences for the model: The number of selectable centrocytes for each shape space state ϕ is given at every time by Eq. (6), i.e. the number of centrocytes just being in the selection process. Furthermore, the details of the multi-step selection process (Lindhout et al., 1997) are omitted. The

selection is modeled by a sum over the shape space of the antigen distribution presented on the FDCs weighted by the affinity function Eq. (1). In other words the centrocytes $gB(\phi)$ are selected if an antigen is close enough in the shape space. The meaning of *close enough* is determined by the width of the affinity function and by the probability a_0 of a positive selection for an optimal centrocyte with respect to one presented antigen.

One should be aware that the probability a_0 is not necessarily equal to one, as centrocytes are in the state of activated apoptosis (Cohen et al., 1992) such that their life time is finite and they have to be selected within this life time to be rescued from apoptosis. This maximum selection probability is determined by the relation of the centrocyte life time of about $10 h$ (Liu et al., 1989, 1994) and the duration of the selection process of $1 - 2 h$ (van Eijk & de Groot, 1999). A rough estimate using two Gaussian distributions with reasonable widths for the life time and the selection time peaked at $10 h$ and $1.5 h$ respectively leads to $a_0 \approx 0.95$. Thus, if a GC contains only centrocytes of optimal complementarity to a presented antigen, still about 5% of them will undergo apoptosis.

In conclusion, selection can be described by the convolution term

$$\sum_{\phi^*} C(\phi) A(\phi^*) a_0 a(\phi, \phi^*) \quad , \quad (7)$$

where the number of selectable centrocytes is given by Eq. (6) and $A(\phi^*)$ represents the distribution of antigens on the shape space. This selection term contributes with probability q to the production of plasma and memory cells

$$\frac{dO}{dt}(\phi) = q \sum_{\phi^*} C(\phi) A(\phi^*) a_0 a(\phi, \phi^*) \quad . \quad (8)$$

All selected centrocytes not emitted from the GC are recycled and in this way enhance the centroblast population giving rise to the last term in Eq. (3).

2.3 Initial conditions

Antigen distribution

Throughout the paper the antigen distribution is assumed unequal to zero at exactly one point in the shape space:

$$A(\phi^*) = A(\phi_0) = \delta(\phi^* - \phi_0) \quad , \quad (9)$$

where $\delta(\cdot)$ is one for its argument equal to zero and zero otherwise. Consequently, the sum in the convolution term in Eq. (3) is reduced to one contribution. This implies that we consider only one type of antigen epitope to be present in the GC. What seems to be a restriction at first sight turns out to be an assumption without any loss of generality. In view of about 10^{11} possible states in the naive repertoire of humans (Berek & Milstein, 1988) two randomly chosen antigen epitopes will not be in direct neighborhood of each others in the shape space. Both antigen epitopes will only have an influence on each other during the GC reaction when centroblasts corresponding to one of the antigen epitopes have a non-negligible affinity to the other epitope. In the shape space language this situation

corresponds to an overlap of two spheres centered at both antigen epitopes. The radius of these spheres is determined by the maximum number of mutations which may occur during a GC reaction. This number will rarely exceed 9 (Küppers et al., 1993; Wedemayer et al., 1997) such that in a 4-dimensional shape space (a more detailed discussion of the shape space dimension follows in Sec. 2.5) one sphere of this size covers about 10^{-8} th part of the space. An overlap is unlikely as an unreasonable large number of 10^8 antigen epitopes is needed to get an important probability for a mutual influence. Therefore we consider one-antigen epitope GC reactions only. A multiple-antigen or a multiple-antigen epitope GC reaction has to be considered as sum of one-antigen epitope GCs.

There exists experimental evidence that the amount of presented antigens is reduced during a GC reaction (Tew & Mandel, 1979). Since the amount of antigen is only halved during 30 days (Tew & Mandel, 1979; Oprea et al., 2000) we do not expect an important recoil effect on the selection probability, which would become time dependent otherwise. Furthermore, we believe that this antigen diminution is too weak to be responsible for the vanishing cell population in GCs after about 3-4 weeks. Anyhow, we aim to show that our three-phase model allows for a vanishing population solely due to the dynamics of the system, without the inclusion of any antigen distribution dynamics.

B-cell distribution

The B-cells which have moved to FDCs are in a fast proliferation phase. In this first phase of GC development the cell population grows exponentially until it has reached about 10^4 cells after three days. One may ask how many seeder cells are necessary and sufficient to give rise to this large cell population within such a short space of time. One finds experimentally that the follicular response is of oligoclonal character (Liu et al., 1991; Jacob et al., 1991; Küppers et al., 1993; Kroese et al., 1987) and the number of seeder cells is estimated between two and six. This result is in accordance with the proliferation rate of $\ln(2)/(6h)$ cited above.

The number of seeder cells $\sum_{\phi} B(\phi, t = 0)$ determines the initial B-cell distribution $B(\phi)$ in our model. Corresponding to the experimental results cited above, we start with the reasonable number of three seeder cells for the follicular response to an immunization with a specific antigen. These cells are chosen randomly in the shape space within a sphere of radius R_0 around the presented antigen. Due to the assumed affinity neighborhood this reflects a threshold affinity of antigen and activated initial B-cells. This was already found experimentally (Agarwal et al., 1998): The activation of a B-cell by an antigen is necessarily connected with a minimum affinity of the corresponding epitopes and antibodies. The radius of the sphere can be determined by the maximum number of mutations occurring during the process of affinity maturation in GCs:

$$R_0 = N_{\max} \quad , \quad (10)$$

which is found to be 8 or 9 (Küppers et al., 1993; Wedemayer et al., 1997). In this picture, B-cells with an affinity above threshold are activated by a specific antigen, giving rise to a fast immune response with antibodies of low but non-vanishing affinity. The germinal center reaction has to be understood as an optimization process for these initially activated B-cells leading to a second slower primary immune response of high specificity.

2.4 Width of affinity function

Due to affinity neighborhood in the shape space the affinity function may be chosen according to Eq. (1). The width Γ has to be consistent with the affinity enhancement that is achieved during a GC optimization process. Let the factor of affinity enhancement be 10^ξ and the number of corresponding somatic hypermutations be N . Then from Eq. (1) we get

$$\Gamma = \frac{N}{(\xi \ln(10))^{\frac{1}{\eta}}} \quad . \quad (11)$$

Typical numbers of somatic hypermutations are $N = 6$ (Küppers et al., 1993) corresponding to an affinity enhancement of 100 ($\xi = 2$) (Janeway & Travers, 1997), while $N = 8$ is considered to be a large number of mutations (Küppers et al., 1993) corresponding to a high factor of affinity enhancement of 2000 ($\xi = 3.3$) (Janeway & Travers, 1997). A huge affinity enhancement by a factor of 30000 ($\xi = 4.5$) is reached with $N = 9$ mutations (Wedemayer et al., 1997). As can be seen in Fig. 2, these values for the affinity enhancement with growing number of somatic hypermutations are consistent with a Gaussian affinity function ($\eta = 2$) with width of $\Gamma \approx 2.8$. It should be mentioned that a consistent

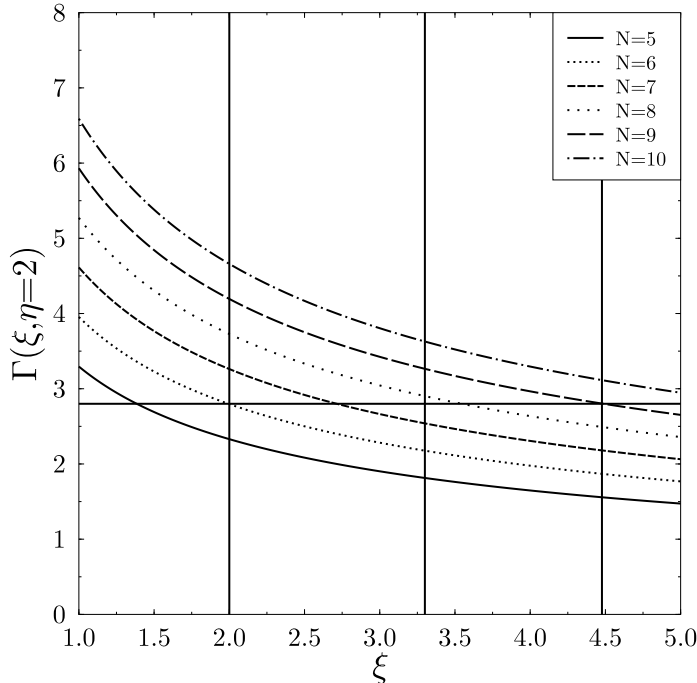


Figure 2: The width of the Gaussian affinity function as a function of the factor of affinity enhancement for different numbers of somatic hypermutations. Vertical lines denote the positions of the used experimental values of affinity enhancement. One can observe that consistently for all three values the resulting width becomes approximately 2.8.

value for the width of the affinity function can not be obtained for other integer values of η . But one should be aware that the used affinity enhancements are very rough estimates and thus our result should be understood as a first guess – even if the compatibility with the experimental data is convincing.

2.5 Shape space dimension

The shape space dimension D enters the model through the mutation term in Eq. (3) and has to be chosen appropriately to our model. We already mentioned that somatic hypermutation is likely to occur randomly (Weigert et al., 1970; Radmacher et al., 1998), i.e. that the direction of mutation in the shape space is not governed by the position of the antigen. The term describing mutation in Eq. (3) is in analogy to a diffusion term in a continuous space as used in (Perelson & Wiegel, 1999). Let us assume for a moment that the development of the GC reaction is governed by a diffusion process and let the number of maximum point mutations be N_{\max} . Then the diffusion process operates in a sphere around a seeder cell of radius N_{\max} in the shape space. In order to match the position of the antigen with at least one centroblast, all positions in the sphere have to be reached by diffusion. This means that the total number of centroblasts N_c present in the GC 3 days after immunization, i.e. when selection is triggered, should be of the order of magnitude of the number of points in the sphere. The number of points in the sphere grows exponentially with the dimension of the shape space. Thus, for $N_{\max} = 8$ and $N_c = 12000$ it follows that the shape space dimension should be 4. From the point of view of a pure diffusion process this is an upper bound for the shape space dimension.

However, the above argument does not include the proliferation rate, the selection rate, and the recycling probability. The effective number of centroblasts available to reach the antigen may become larger than the 12000 cells assumed above through proliferation and recycling. As we want to describe a decreasing population for large times without further assumptions, the effective rate of production of additional centroblasts during the GC reaction cannot exceed some small value, since the centroblast population would explode otherwise for large times. So it seems unlikely that the shape space dimension appropriate for our model is substantially larger than 4. We will start with $D = 4$ and check our results for the dimensions 5 and 6. We want to remind that we are dealing with a phenotype space in this model and that a genotype space probably requires a substantially higher dimension.

2.6 Long term behavior

The parameter g was introduced in the model as the rate of differentiation from centroblasts in the dark zone into antibody presenting centrocytes ready to undergo a selection process. As we do not consider the centrocyte dynamics during the multi-step selection process (Lindhout et al., 1997), this parameter effectively describes the total duration of the selection process including the differentiation mentioned above, the selection at the FDCs and with T-helper cells, and the recycling to centroblasts. Only those cells that have successfully finished this program are contributing to the centroblast population described in Eq. (3).

Thus, being an effective measure of the speed of the selection process, we are able to deduce an upper bound for g . Solely the inhibition of apoptosis during the selection process at FDCs and with T-helper cells takes at least 1-2 hours (Lindhout et al., 1995; van Eijk & de Groot, 1999). This gives us an upper bound for the rate g of

$$\frac{g}{\ln(2)} < \frac{1}{2h} . \quad (12)$$

Nevertheless, this upper bound is not sufficient to fix g . As g governs the whole reaction speed it will play a crucial role for the final state 21 days after immunization. As we know that at the end of the GC reaction only a few cells remain in the environment of the FDCs (Liu et al., 1991; Kelsoe, 1996), the parameter g will be tuned in order to get this result.

Mathematically, this requirement has the form of a long term condition. Let us look for an equilibrium condition at the point ϕ_0 representing the antibody type of optimal complementarity to a presented antigen:

$$\frac{dB}{dt}(\phi = \phi_0, t) = 0 \quad . \quad (13)$$

Then, the selection term in Eq.(3) becomes simply $(1 - q)ga_0B(\phi_0, t)$ and for a non-vanishing centroblast distribution at ϕ_0 we get

$$\varepsilon \equiv p - 2pm - g + \frac{pm\beta}{D} + (1 - q)ga_0 = 0 \quad , \quad (14)$$

where we have introduced ε as a measure for the vicinity to the equilibrium condition and

$$\beta(\phi_0, t) = \frac{\sum_{\|\Delta\phi\|=1} B(\phi_0 + \Delta\phi, t)}{B(\phi_0, t)} \quad . \quad (15)$$

$\beta(t)$ is a measure for the sharpness of the centroblast distribution in the shape space around the antigen position ϕ_0 . β becomes constant when the selection process starting at day 3 after immunization has reached a phase in which the centroblasts at the position of the antigen dominate. This is already the case 8 days after immunization according to experiments (Jacob et al., 1993) and is confirmed in our model (see Fig. 6).

Thus, at large times β can already be considered as constant in the equilibrium condition Eq. (14) and the same applies to ε . In this stage of GC development the centroblast population at ϕ_0 has a pure exponential form

$$B(\phi_0, t) = e^{\varepsilon t} \quad . \quad (16)$$

The sign of ε determines whether the centroblasts population explodes ($\varepsilon > 0$) or dies out ($\varepsilon < 0$). Because of the finite life times of GCs, ε should adopt values slightly smaller than zero.

2.7 Recycling probability

The recycling probability $1 - q$ determines the fate of the positively selected centrocytes in the light zone. Apoptosis was inhibited for these cells and they may either become plasma or memory cells or return to the dark zone to reenter the fast proliferation phase. This recycling hypothesis (Kepler & Perelson, 1993) has been intensively discussed and the main position is that random somatic hypermutation – and it is likely that somatic hypermutation occurs randomly (Weigert et al., 1970; Radmacher et al., 1998), i.e. that the direction of mutation in the shape space does not depend on the position of the antigen – does not lead to a sustained optimization of affinity in a one-pass GC reaction (Oprea

et al., 2000). To reach a specific position in the shape space a multi-step optimization and verification process is required to avoid an arbitrary aimless walk through this high dimensional space.

To propose a new perspective onto this question we consider the most convincing experimental evidence for the existence of such a recycling process (Han et al., 1995b). A GC reaction was initiated in mice with one antigen. 9 days after immunization, i.e. in a stage of the reaction in which the *good* cells already dominate (Jacob et al., 1993), a second different, but related antigen was injected. This change of the reaction conditions in the course of the GC reaction leads to some very interesting observations: The rate of apoptosis of centrocytes is enhanced by a factor of about $\nu \approx 5$ compared to the non-disturbed GC reaction. This can be explained by the fact that the antigen distribution in the shape space was changed such that most of the cells present after 9 days may fit to the first antigen but not to the second one. The probability of a positive selection is diminished and the inhibition of apoptosis does not occur to the same extent as before. On the other hand the total cell population in the GC vanishes with a $\omega \approx 8$ -fold higher speed compared to the unperturbed GC reaction. This is very difficult to explain without recycling: As we know that the centrocytes (only very small numbers of centroblasts) undergo apoptosis if not rescued in time, the change of the apoptosis rate is of relevance only for the centrocyte population. The faster reduction of the whole GC cell population can not be explained by the enhanced apoptosis rate, if there exists no recoil effect of the centrocyte apoptosis to the centroblast population. This is an indirect confirmation of the recycling hypothesis.

We want to consider this argument in a quantitative way by translating this experiment into the language of our model. We know from our consideration in Section 2.6 that at day 9 after immunization the optimization process is already completed and that the centroblast population at the antigen position $\phi = \phi_0$ in the shape space behaves according to Eq. (16). But due to the modification of the antigen distribution at day 9 after immunization the GC reaction returns back to its dynamical selection phase. Thus, until day 9 the centroblast population $B_1(\phi, t)$ evolves with respect to the antigen distribution $A_1(\phi^*)$ as in Eq. (9) and after day 9 two GC developments have to be compared: One continues its usual reaction as before. The second $B_2(\phi, t)$ starts with the distribution $B_1(\phi, t = 9d)$ and evolves with respect to the new antigen distribution

$$A_2(\phi^*) = \rho_1 \delta(\phi^* - \phi_0) + \rho_2 \delta(\phi^* - (\phi_0 + \Delta\phi^*)) \quad , \quad (17)$$

where $\Delta\phi^*$ denotes the shift of the additional second antigen with respect to the first one. $\rho_{1,2}$ take into consideration the (possibly) different concentrations of both antigens.

Now we are able to calculate the apoptosis rate in both scenarios for the cells of some fixed but arbitrary type ϕ . The number of centrocytes available for selection at every moment is $gB(\phi)$. The apoptosis rate is given by this number reduced by the selected cells

$$V_i(\phi) = gB(\phi) \left(1 - a_0 \sum_{\phi^*} A_i(\phi^*) a(\phi - \phi^*) \right) \quad , \quad (18)$$

where i denotes the two scenarios. For the original GC reaction this becomes

$$V_1(\phi) = gB(\phi) (1 - a_0 a(\phi - \phi_0)) \quad , \quad (19)$$

while in the GC with the new antigen distribution we find

$$V_2(\phi) = gB(\phi) (1 - a_0 a(\phi - \phi_0) \rho_1 (1 + \alpha(\phi))) \quad , \quad (20)$$

where we have shifted ϕ^* in the second term of Eq. (17) and introduced the ratio

$$\alpha(\phi) = \frac{\rho_2 a(\phi - \phi_0 - \Delta\phi^*)}{\rho_1 a(\phi - \phi_0)} \quad (21)$$

valid for each point ϕ separately. The factor ν of the apoptosis enhancement found in the experiment above is then given by the ratio of both apoptosis rates

$$\nu = \frac{V_2}{V_1} = \frac{1 - a_0 a(\phi - \phi_0) \rho_1 (1 + \alpha(\phi))}{1 - a_0 a(\phi - \phi_0)} \quad . \quad (22)$$

On the other hand, this enhancement of apoptosis leads to a faster population reduction by a factor ω , which in our model is given by the ratio of the changes of the cell distributions over the shape space at the time of the presentation of the new antigen. According to Eq. (3) and using the new antigen distribution A_2 this ratio is given by

$$\begin{aligned} \omega &= \frac{dB_2}{dt} \left[\frac{dB_1}{dt} \right]^{-1} (\phi, t = 9d) \\ &= \frac{p - 2pm - g + \frac{vm}{D} \beta(\phi) + (1 - q)ga_0 a(\phi - \phi_0) \rho_1 (1 + \alpha(\phi))}{p - 2pm - g + \frac{vm}{D} \beta(\phi) + (1 - q)ga_0 a(\phi - \phi_0)} \quad , \quad (23) \end{aligned}$$

where the cell distributions $B(\phi, t = 9d)$ cancel as they are equal in both scenarios for $t = 9d$.

Taking the results for ν (Eq. (22)) and for ω (Eq. (23)) at the shape space point of the primary antigen $\phi = \phi_0$ the affinity function becomes equal to one. β is already a constant for $t = 9d$ such that we may eliminate $\rho_1(1 + \alpha(\phi_0))$ from both equations to get

$$\frac{\nu - 1}{\omega - 1} = \frac{p - 2pm - g + \frac{vm}{D} \beta(\phi_0) + (1 - q)ga_0}{(1 - q)g(a_0 - 1)} \quad (24)$$

or for the recycling probability

$$1 - q = -\frac{p - 2pm - g + \frac{vm}{D} \beta(\phi_0)}{g \left[a_0 + (1 - a_0) \frac{\nu - 1}{\omega - 1} \right]} \quad . \quad (25)$$

This relation allows us to determine the parameter q and in this way to give a quantitative prediction for the recycling probability for selected centrocytes to reenter the dark zone and to continue proliferation. The recycling probability has to fulfill Eq. (25) in order to be consistent with the experiment of Han et al., (1995b). We want to emphasize, that the condition Eq. (25) is independent of the concentrations of the two antigen types used in the experiment.

2.8 Output dynamics

The production of plasma and memory cells optimized with respect to the presented antigen in the course of the GC reaction is governed by Eq. (8). According to our discussion of the different phases of the GC reaction in Sec. 2.2, the starting time of *output cell* production is not necessarily correlated with the starting time of the mutation and selection process about 3 days after immunization. There may occur a time delay of the output production in relation to the selection process (see Fig. 1). This possibility is encountered by comparing the dynamics of output cell production with experiment (Han et al., 1995a). Here, the number of output cells of high affinity to the presented antigen ϕ_0 is compared at day 6 and day 12 after immunization and their relation is found to be approximately

$$v_O \equiv \frac{\int_{0d}^{12d} dt O(\phi_0)}{\int_{0d}^{6d} dt O(\phi_0)} \approx 6 \quad . \quad (26)$$

As output cells are already present at day 6 after immunization, the starting point of output cell production has to fulfill $0 h < \Delta t_2 < 72 h$ (Δt_2 denotes the time window between the start of mutation and selection and the start of output cell production, see Fig. 1). It is intuitively clear that for large Δt_2 the speed of output cell production v_O will be enhanced, for the cell population of the GC will already be peaked at the position of the antigen in the shape space. Thus, we are able to adjust Δt_2 to the correct output cell dynamics.

3 Results and Predictions

Parameter	quantity = value
Proliferation rate	$p / \ln(2) = 1 / (6 h)$
Somatic hypermutation probability	$m = 0.5$
Rate of differentiation of centroblasts to centrocytes	$g / \ln(2) = 0.352$
Dimension of shape space	$D = 4$
Selection probability for optimal centrocytes	$a_0 = 0.95$
Output probability of selected centrocytes	$q = 0.2$
Number of seeder cells at FDCs	$\sum_{\phi} B(\phi, t = 0) = 3$
Radius of B-cell activation around antigen	$R_0 = 8 - 10$
Time duration of phase I of GC reaction	$\Delta t_1 = 72 h$
Time duration of phase II of GC reaction	$\Delta t_2 = 48 h$
Time duration of the whole GC reaction	$\sum_{i=1}^3 \Delta t_i = 504 h$

Table 2: Summary of all parameters of the model. They were determined by experimental data. For explanations and references see the last section. The parameters g , q , and Δt_2 are determined in the course of the solution of Eq. (3) with respect to experimental data discussed before.

Starting from a randomly chosen antigen epitope and – following the oligoclonal character of the B-cell population of a GC – three randomly chosen activated B-cells in a sphere

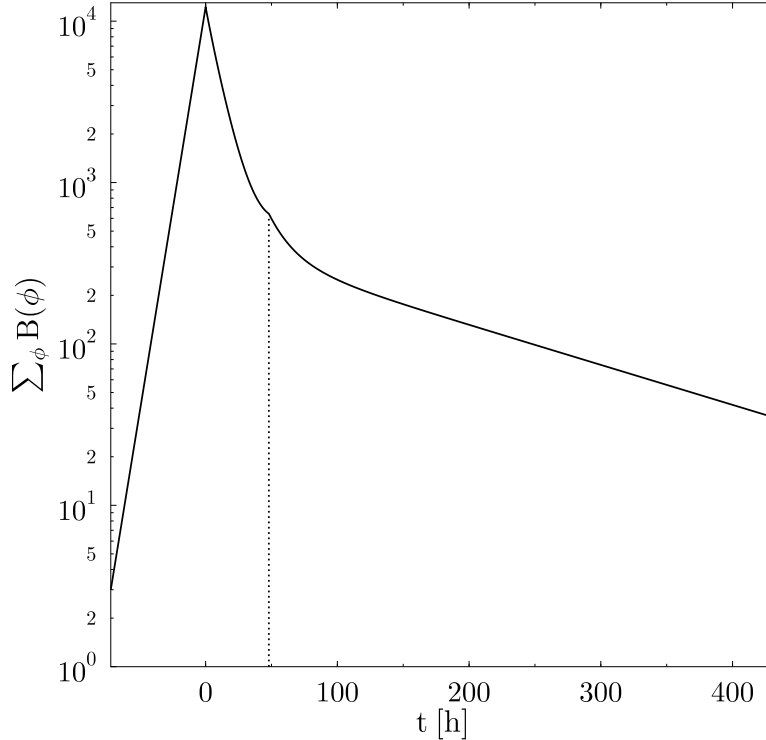


Figure 3: Time course of the centroblast population integrated over the whole sphere in the shape space around the antigen ϕ_0 . In the first phase the initial B-cells proliferate. The large population reached at $t = 0 h$ is then reduced by the selection process. At $t = 48 h$ the production of plasma and memory cells starts, leading to an exponential decrease in the overall centroblast population.

of radius R_0 according to Eq. (10), we let the GC reaction develop as described by Eq. (2) and Eq. (3). The different phases (see Sec. 2.2) of the GC reaction are respected. The parameters are determined from experimental data as summarized in Tab. 2. The parameters g , $1 - q$ and Δt_2 , describing the differentiation rate of centroblasts to centrocytes, the recycling probability for the selected centrocytes and the time delay for the production of output cells, respectively, are iteratively adjusted in order to fit with the experiments described in the previous section. The time variable is running from $t_0 = -72 h$ to accentuate the first phase of pure proliferation as a *preGC-phase*. The mutation and selection process is started at $t = 0 h$ and the production of plasma and memory cells begins at $t = \Delta t_2$. The differential equation is solved numerically with a modified Euler method in a subspace, in which we assume Dirichlet boundary conditions with $B = 0$.

The best results are obtained by an iteration procedure for

$$\frac{g}{\ln(2)} = \frac{0.355}{h} \quad , \quad 1 - q = 0.8 \quad , \quad \Delta t_2 = 48 h \quad . \quad (27)$$

At $t = 0 h$ we find a large oligoclonal population of 12288 centroblasts as a result of the proliferation phase started with 3 initial cells (see Fig. 3). These cells are of different type compared to the cells of optimal affinity to the presented antigen and in a typical distance

from them (varying between 3 and 8 point mutations to reach the optimal cell type).

Optimization phase The selection process at the FDCs and with the T-helper cells starts and reduces the centroblast population with low affinity to the presented antigen. At the same time somatic hypermutation leads to a spreading of the centroblast distribution over the shape space, resulting in a small but non-vanishing amount of centroblasts at the shape-space position of the antigen (see Fig. 4). The large majority of B-cells does not

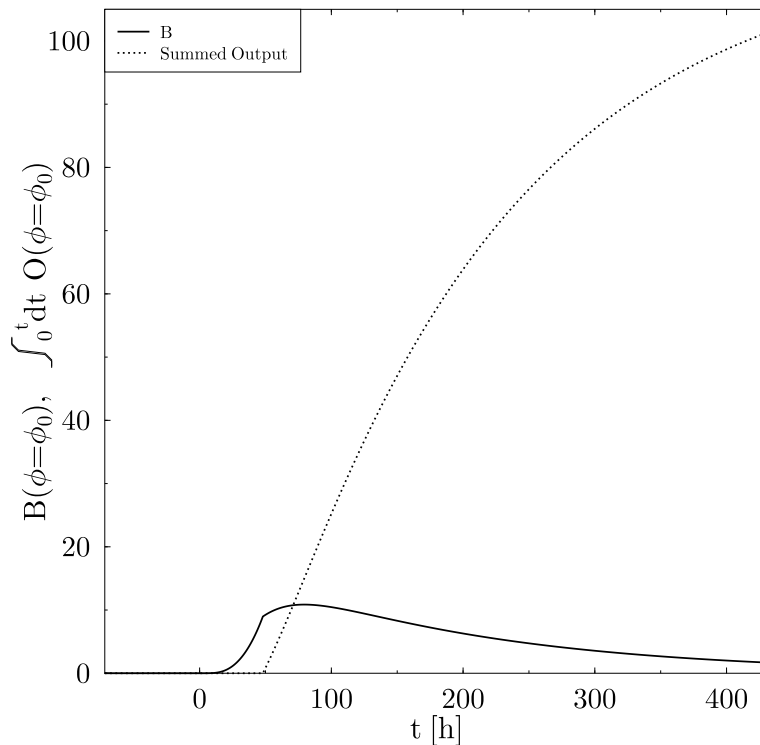


Figure 4: The centroblast population and the integrated plasma/memory cell production at the position of the antigen in the shape space. The centroblast population shows a growth due to proliferation and somatic hypermutation starting at $t = 0 h$. The population growth is slowed down by the production of output cells starting at $t = 48 h$. Now the number of produced plasma and memory cells is increased steadily until the end of the GC reaction. Then, only 2 cells (of optimal type) remain in the environment of the FDCs.

survive the selection process (compare the summed cell population decrease in Fig. 3), dies through apoptosis and is rapidly phagocytosed by macrophages present in the GC.

Secondary proliferation As all positively selected centrocytes reenter the proliferation process in the optimization phase of the GC reaction, the number of centroblasts at the antigen position grows. Note that $\varepsilon > 0$ follows for the equilibrium condition Eq. (14) because of $q = 0$, according to Eq. (4). As a consequence, the overall centroblast population would restart to grow if this growth was not inhibited by the production of plasma and memory cells after $48 h$. Especially, this *secondary proliferation* process is found for the

centroblasts encoding antibodies of high affinity to the antigen (see Fig. 4). The centroblasts at the antigen position are practically all recycled (beside the reduction due to $a_0 < 1$) such that no reduction process exists any more. This gives rise to a new perspective on the GC reaction: We need just as many initially proliferated cells, that a spreading of the distribution through somatic hypermutation leads to at least one or two cells matching the antigen position in the shape space. Then a considerable amount of cells of this optimized type is reached within the time delay Δt_2 of the production of output cells, opening the possibility of a full proliferation process for these cells.

Recycling probability When the output production is turned on at $t = 48 h$ the dynamics of the germinal center is characterized by $\varepsilon < 0$ in Eq. (14), such that an exponential decrease of the whole centroblast population is initiated – including the population of the optimized cells (see Fig. 3 and Fig. 4). Nevertheless, this decrease is slow enough to allow the production of a considerable amount of plasma and memory cells (see Fig. 4 and Fig. 5). It is an interesting observation that a rather small number of centroblasts of the optimal

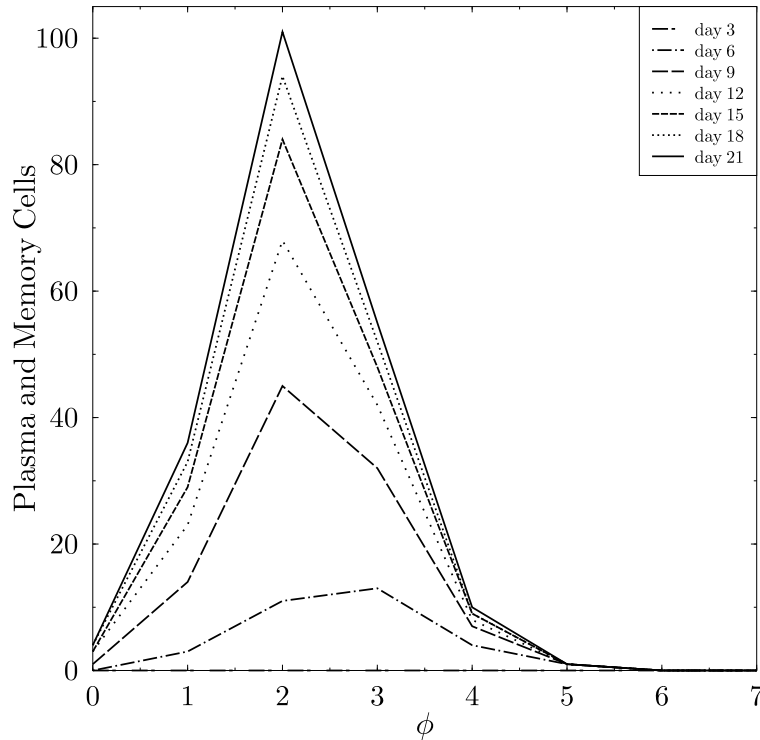


Figure 5: A cut through the sphere in the shape space around the presented antigen at position 2. The seeder cells are at a distance of at least 5 mutation steps. The number of produced plasma and memory cells grows considerably during the GC reaction. The rapidity of growth diminishes in course of time because of the decreasing number of optimized centroblasts at the antigen position.

type with respect to the antigen is sufficient to produce this large number of plasma and memory cells – even with a small output probability of $q = 0.2$. On the contrary, a larger

output probability may decrease the integrated number of plasma and memory cells, as less cells reenter the proliferation process. In conclusion, we claim that a large recycling probability of 80% of the positively selected centrocytes is not only necessary to achieve an optimization by multi-step mutations but also to achieve a high number of resulting plasma and memory cells.

The end of the GC reaction Finally, at day 21 after immunization, only a few cells with maximum affinity to the antigen remain in the environment of the FDCs, as required from experiment (Liu et al., 1991; Kelsoe, 1996). So the dynamics of our model allow for a vanishing of the germinal center population without any reduction of the antigen concentration or other additional requirements. The length of the germinal center reaction is determined by the interplay of the centroblast (into centrocyte) differentiation rate g and the delay of output production Δt_2 , which is determined by Eq. (26), so that the GC life time is basically controlled by g . So from the perspective of our model a diminishing cell population may result solely from the interplay of proliferation, differentiation of centroblasts to centrocytes, and output production.

Dependence of initially activated seeder cells The total number of remaining cells depends on the distance of the initial B-cells from the antigen ϕ_0 . For numbers of mutation steps (necessary to reach the antigen) between $N = 3$ and $N = 8$, the number of remaining B-blasts varies from 43 to 0. For a typical number of mutations of $N = 5$ about 10 B-blasts remain in the environment of the FDCs at day 21 after immunization. In other words, the GC life time depends on the initial distribution of the seeder cells with respect to the presented antigen. It would be interesting to check this statement experimentally by observing GCs with a variable number of mutations occurring during the optimization process. One could imagine for real GCs a self-regulating process which depends on the already positively selected centrocytes and thus prolongs the GC reactions with large distances between seeder cells and antigen, and shortens correspondingly the ones with small distances. However, there is experimental evidence that the intensity of the GC reaction depends on the quality of the initially activated B-cells (Agarwal et al., 1998). Also in quasi-monoclonal mice (Cascalho et al., 1996) it was found that the volume of GCs 4 days after immunization depends on the average affinity of the reservoir B-cells to the antigen (de Vinuesa et al., 2000, Fig. 6). A quantitative comparison of these data with our model results would be interesting.

3.1 Result stability

The parameter set in Eq. (27) is determined such that the experimental conditions Eq. (25) and Eq. (26) are fulfilled for typical initial conditions. Therefore, the prediction of the recycling probability to be 80% is a statement which – in the framework of our model – is justified to the same degree as the experiments are exact. Nevertheless, the sensitivity of the predicted high recycling probability to such modifications is weak.

It should be mentioned that in addition there is a certain freedom of choice concerning the number of remaining cells at day 21 after immunization. For example, the parameter

set with a still higher recycling probability

$$\frac{g}{\ln(2)} = \frac{0.52}{h} \quad , \quad 1 - q = 0.9 \quad , \quad \Delta t_2 = 55 h \quad . \quad (28)$$

leads to a result of comparable quality as under the conditions of Eq. (27) – it is clear that a higher recycling probability slows down the production of output cells such that simultaneously the time delay of the production start has to be larger – with the difference that the number of remaining cells is reduced with respect to the previous result such that no cells remain at the end of typical GC reactions. For this reason and because g is on its upper bound Eq. (12), this parameter set was not considered as reasonable.

If one requires a smaller recycling probability the parameter set

$$\frac{g}{\ln(2)} = \frac{0.286}{h} \quad , \quad 1 - q = 0.7 \quad , \quad \Delta t_2 = 42 h \quad . \quad (29)$$

leads to correct values for v_0 and Eq. (25) is also fulfilled. The reduced recycling probability accelerates the output cell production such that it has to be decelerated by a reduction of the time delay Δt_2 . Even if the differentiation rate stays in a reasonable range, the number of remaining cells in the GC at day 21 after immunization is about ten-fold with respect to Eq. (27). More generally one may consider the number of remaining cells for typical GC reactions with an average number of mutations necessary to reach the antigen.

Recycling probability $1 - q$	0.5	0.6	0.7	0.8	0.9
$\sum_{\phi} B(\phi, t = 21 d)$	1476	515	134	10	0

The mentioned experimental data are all reproduced for each value of $1 - q$, solely the number of remaining cells is left open. To ensure that this number is in accordance with the experimental statement that *a few* proliferating B-blasts remain at the FDCs at this stage of GC development, we are led to a recycling probability of 80%. We want to emphasize that this result is determined very clearly, as for the other recycling probabilities the remaining number of cells in the GC final state differs by at least an order of magnitude.

This variation of parameters shows the range of stability of our prediction:

First, the window of possible time delays Δt_2 , which are in accordance with Eq. (26) is very narrow. Already for $\Delta t_2 > 55 h$ the condition Eq. (12) will be violated. On the other hand for $\Delta t_2 < 38 h$, despite the immense number of remaining cells in the final GC state, the condition Eq. (26) can not be fulfilled anymore. In consequence, it is not possible that the production of plasma and memory cells already starts with the establishment of light and dark zone, i.e. that it starts with the existence of a fully developed GC. The emphasized experimental bounds require necessarily a time delay for the production of output cells of at least $42 h$. This means that the production process should be initiated by a separate signal and is not present in a working GC automatically.

Secondly, the window of possible recycling probabilities is strongly bound by the experiments (Han et al., 1995a, 1995b) and by the experimentally observed number of remaining cells at day 21 after immunization. This leads to the conclusion that the recycling probability should be at least 70% and not larger than 85%. Even ignoring the required number of cells in the final state, Eq. (26) does not allow a recycling probability smaller than 60%.

We would like to emphasize that this result differs extremely from the value for the recycling probability of 0.15 assumed in (Kesmir & de Boer, 1999). Nevertheless, we do not regard this discrepancy as a contradiction because in the model of Kesmir & de Boer not all parameters were fixed by experimental data.

Shape space dimension The analysis presented above was performed with a shape space dimension of 4, (compare Sec. 2.5). It is an important remark that our results remain essentially unaffected for $D = 5$ or 6. Using for instance $D = 5$, only the parameter g , controlling the selection speed, has to be reduced slightly by 7% in order to stay in accordance with the experimental bounds. The total number of remaining cells at day 21 after immunization does not change but its distribution is spread out on the shape space. For $D = 6$, the parameter g is again reduced by 6%, while all other parameters remain unchanged to stay in accordance with the experimental data. Again, the cell distribution at day 21 after immunization becomes less centered at the antigen position. We conclude that, for the values tested, the dependence on the shape space dimension is weak enough such that our results are not affected by it. Even, the slower selection speed for higher dimensions of less than 10% per dimension remains in the range of accuracy of our results.

Note, that the dependence on the shape space dimension is restricted to an intermediate stage (phase II) of the GC reaction. In the first phase of pure proliferation D does not enter the dynamics at all. In the late phase of selection, when the distribution $B(\phi)$ becomes approximately spherically symmetric around the point representing the antigen, D cancels exactly with the factor $1/D$ in Eq. (3) as there are D equal terms contributing to the sum such that D factorizes. A dependence of our results on the shape space dimension may only occur during the early phase of selection, in which the distribution $B(\phi)$ is clearly not symmetric around the position of the antigen. Since the distribution of centroblasts develops into a spherically symmetric distribution around ϕ_0 already before day 8 after immunization (see Fig. 6), we deduce that a dependence on the shape space dimension may occur between day 3 and day 8 of the GC reaction only.

Mutations with large changes of affinity We have assumed so far that mutations are represented in the shape space by next-neighbor jumps. To check the robustness of the result for the recycling probability against the possibility of mutations that lead to large distance jumps in the shape space, we consider a worst case argument. Let us suppose that 10% of the mutations lead to a large jump in the shape space. This is translated into the model by reducing the number of next-neighbor-mutations by a factor of 0.9. The result is a lower efficiency of the mutation process as the probability for a random mutation to improve affinity with respect to the antigen is very small. Therefore, the final number of cells is reduced by a factor of 10, and the centroblast to centrocyte differentiation rate has to be adjusted (from 0.244 to 0.255) in order to fulfill condition Eq. (25). A similar result as before is obtained by an adjustment of the recycling probability from 0.8 to 0.78. As this is a worst case argument, we consider our result as robust against large jump mutations.

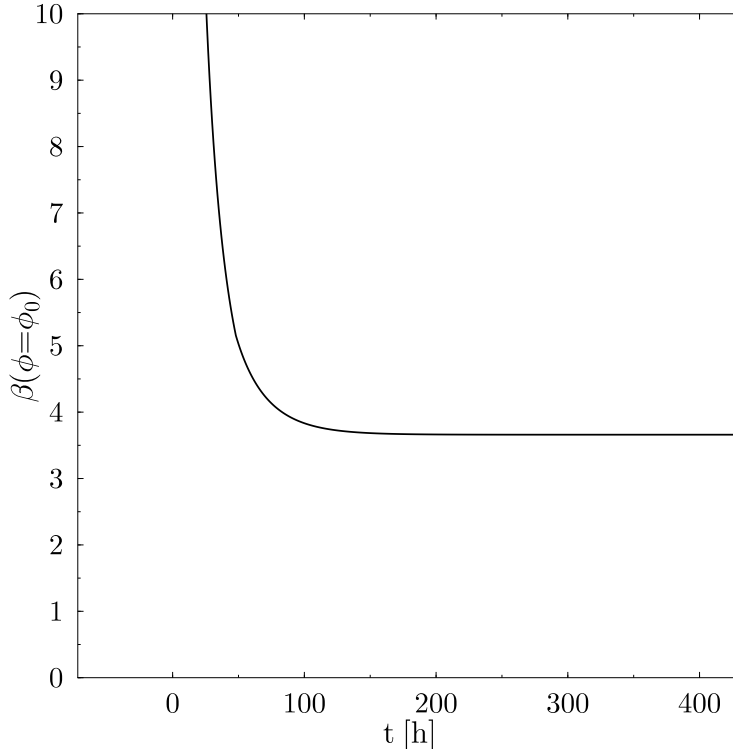


Figure 6: The time course of $\beta(\phi_0, t)$ (see Eq. (15)) at the shape space position of the antigen for the parameter set Eq. (27). β becomes constant shortly after $t = 96$ h, i.e. at day 7 after immunization.

3.2 Optimization speed

From experiment it is expected that the cells with high affinity to the antigen dominate already at day 8 after immunization (Jacob et al., 1993). This is verified in the model by checking if the asymptotic regime of the GC reaction is reached at day 8 in the sense that β (defined in Eq. (15)) becomes constant. As can be seen in Fig. 6, β becomes constant in the course of day 7 after immunization for the parameter set Eq. (27). This behavior of β is not altered in a great range of parameter variation. Besides the reproduction of the experimental evidence for the optimization process to be accomplished after 8 days, this result is an a-posteriori check for the derivation of the recycling probability, which is based on a constant value of $\beta(\phi_0)$ at day 9 after immunization (see Eq. (24)).

3.3 Optimization quality

It may be interesting to verify if larger or smaller recycling probabilities lead to better optimization of the antibody types. The statement that recycling may be necessary to achieve a considerable affinity enhancement in a multi-step mutation process is widely discussed (Oprea et al., 2000) and enforced by the present work. We would like to point out that the relative number of *good* outcoming plasma or memory cells increases with larger recycling probabilities (see Fig. 7). In the shape space this corresponds to a sharper peak

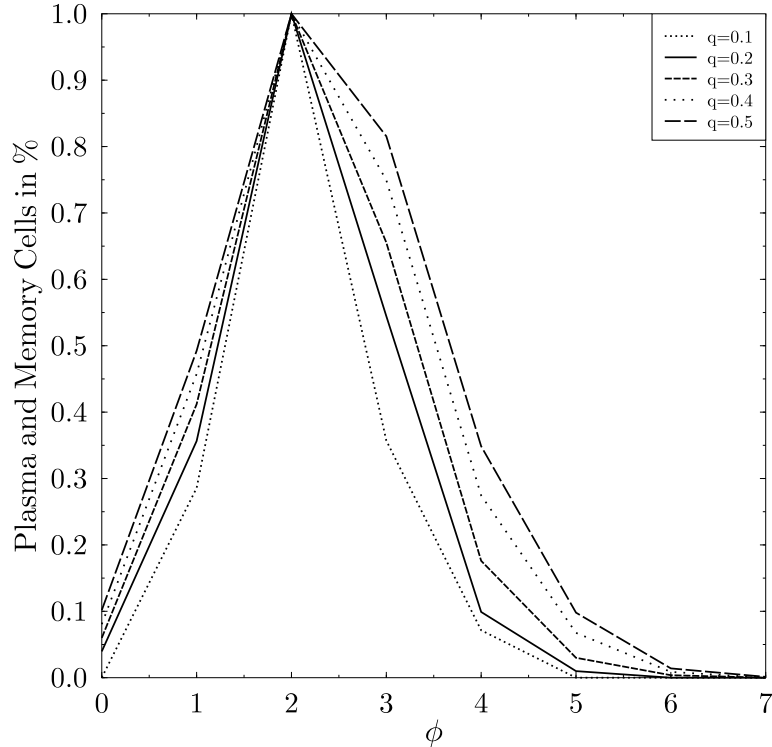


Figure 7: Comparison of the total plasma and memory cell distribution at day 21 after immunization on a cut along one of the coordinates in the shape space with the antigen at coordinate position 2. The parameters are uniquely determined by the experimental data with the exception of the remaining number of cells at the end of the GC reaction, which is undetermined to allow different recycling probabilities $1 - q$. The distribution of the output cells becomes sharper for larger $1 - q$.

of the distribution $\int_0^{21} dt O(\phi, t)$. A too small recycling probability leads to a spreading of the outcoming plasma and memory cells in the shape space, i.e. to a weaker specificity of the GC output.

On the other hand, we have already seen that a larger recycling probability lowers the absolute number of produced plasma and memory cells such that we are confronted with two competitive tendencies. Large recycling probabilities lead to specific but weak GC reactions, while small probabilities lead to unspecific but intense GC reactions. One may agree, that the value of 80% calculated here and supported by experimental data, is a good compromise between these two extremes.

3.4 Start of somatic hypermutation

There is experimental evidence that somatic hypermutation does not occur during the first phase of proliferation of centroblasts in the environment of the FDCs (Han et al., 1995b; Jacob et al., 1993; McHeyzer-Williams et al., 1993; Pascual et al., 1994b). However, we checked if our model allow somatic hypermutation to start during the proliferation phase. The primary reason for the retardation of the output production is to give time to the GC

to develop sufficient good centroblasts before the GC population is weakened through an additional output. Therefore, one may in principle think of a mutation starting long before the selection process. In this scenario the output production would start simultaneously with selection and one is led to a two phase process only: A first one with proliferation and somatic hypermutation and a second one with additional selection and output production. The centroblast-types would already be spread out in the shape space when selection and output start. There is no parameter set in accordance with all experimental data.

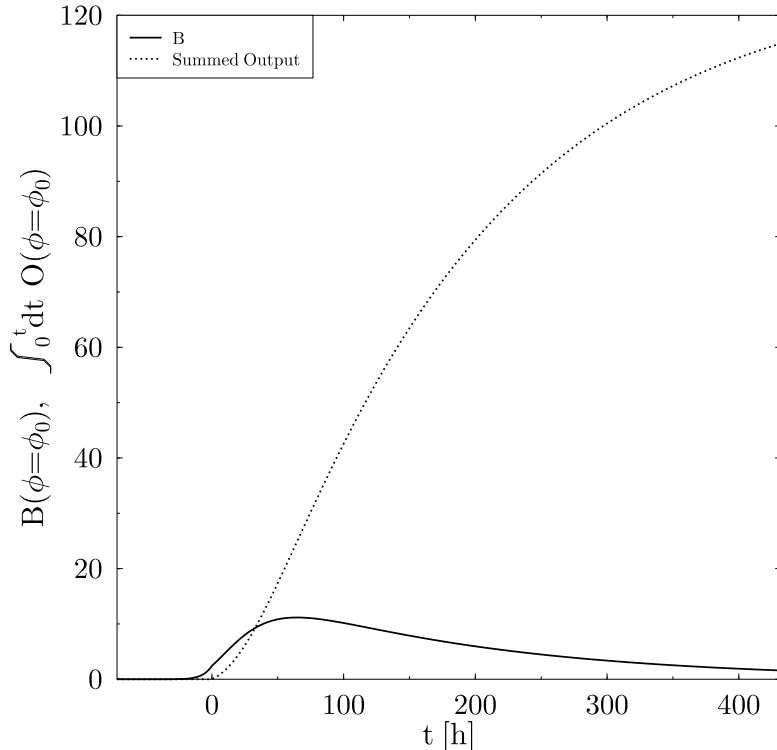


Figure 8: The centroblast population and the integrated plasma/memory cell production at the position of the antigen in the shape space. Except for the time phases we used the same parameters as in Eq. (27). The centroblast population shows a smooth enhancement due to somatic hypermutation starting at $t = -48 h$. The population growth is stopped by the production of output cells starting at $t = 0 h$. The slope of the summed output is substantially smaller than expected from experiment. 21 days after immunization only 1 cell remains.

Especially, it is impossible to get the correct output dynamics as described in Eq. (26). Typically we get $v_0 = 2.9$ being strongly different from the required value and a much smoother result (compare Fig. 8 to Fig. 4). In addition the distribution of plasma and memory cells is not as well pronounced at the antigen position such that the GC reaction gives rise to output cells with weaker specificity. Thus, we deduce from our model that the dynamic of plasma and memory cell production in real GC reactions does not allow somatic hypermutation to occur considerably before the selection process is started.

4 Conclusions

We developed a new model for the GC reaction using its main functional elements. The GC reaction is described by the evolution of a centroblast distribution on an affinity shape space with respect to an initially fixed antigen distribution. On this shape space an affinity function, modeling the complementarity of antibody and antigen, was defined and its functional behavior as well as its width were deviated from affinity enhancements known for real GC reactions.

In the model the reaction is decomposed into three phases (see Fig. 1). In the proliferation phase a few seeder cells multiply. Our model excludes somatic hypermutation to occur already at this stage of the GC development. An optimization phase follows, in which in addition to proliferation, mutation of the antibody type and selection take place. This leads to a competition of spreading and peaking of the centroblast distribution in the shape space. In this phase, all positively selected cells reenter the proliferation phase in the dark zone, i.e. no plasma or memory cells are produced. This occurs solely in the output production phase. In this third phase all elements of the GC reaction are active.

The dynamical evolution of the cell population in a GC is described by a set of coupled linear differential equation. All parameters are determined with experimental data and especially using (Han et al., 1995b). The model shows the typical behavior of GCs without any further adjustments. Due to the oligoclonal character of GCs a large amount of identical centroblasts is produced in the proliferation phase. These diffuse over the shape space in the second phase, in which only those cells are retained that exhibit a high affinity to the presented antigen. As the *good* cells reenter the proliferation process, this leads to a dominance of good cells within 7 to 8 days after immunization in accordance with experiments. The already optimized cell distribution then gives rise to plasma and memory cells leaving the FDC environment in the output production phase, leading to large numbers of output cells of optimized type due to the long duration of this third phase. The GC reaction is rather weak 21 days after immunization and only a small number of cells remains in the environment of the FDCs. This shows that the end of a GC reaction is not necessarily coupled with an antigen consumption or additional signals, but may occur simply due to the (unchanged) dynamical development of the GC.

Our main result is that the experimental data and especially the evaluation of (Han et al., 1995b) lead to the following view of the GC reaction. The optimization phase lasts for not less than 42 *h* and not longer than 55 *h*. During this time *all* selected centrocytes are recycled and reenter the proliferation phase. Without such a *non-output phase* the number of optimal cells with respect to the presented antigen is not large enough to allow a considerable output rate during the remaining life time of the GC. We looked for an experimental evidence for this delayed production of output cells. Indeed, comparing two experiments (Jacob et al., 1993; Pascual et al., 1994a) we found that plasma and memory cells were first observed more than two days later than mutated cells during a GC reaction. This confirms experimentally the existence of the non-output phase that we found in the model. As output cells are not produced from the beginning of the GC reaction, the output should be triggered by a special signal, related to the affinity of the B-cells and the corresponding antigen. But even in the output production phase, the recycling probability turns out to lie between 70% and 85% and thus is substantially larger than

values expected until now (Kesmir & de Boer, 1999). We want to emphasize that such large recycling probabilities turned out to be crucial for a GC outcome of high specificity. Larger recycling probabilities lead to specific GC reactions of low intensity, while smaller ones to less specific but more intense GC reactions. The value of about 80% that we found represents a good compromise between these competitive tendencies. On the other hand it is not surprising that these recycled cells have not been found experimentally: The absolute number of recycled cells is very small compared to the total number of cells present in the GC, so that a measured signal for recycled cells is suppressed by more than two orders of magnitudes. A better signal should be observed in later stages of the GC reaction when the cells of high affinity to the antigen are already dominating.

Furthermore, we conclude that the whole selection process including differentiation of centroblasts to antibody presenting centrocytes, the multi-step selection process itself and finally the recycling take around 3 or 4 *h*. This result is compatible with the experimental observation that the inhibition of apoptosis during the selection may take about 1 or 2 *h*.

It is interesting, that the produced cells possess a certain broadness in the shape space, i.e. not only the centrocytes of optimal affinity to the antigen differentiate to plasma and memory cells. This may be of relevance for the resistance of an immune system against a second immunization with a mutated antigen. A considerable number of memory cells with high affinity to the mutated antigen may still be present for this reason.

The results of our model suggest new experiments. A systematic and quantitative analysis of the GC reaction in dependence of the initial conditions, i.e. the number of necessary point mutations to reach the cell type of optimal affinity to the antigen, would lead to new insights into the interdependence of the essential elements of the GC. This may yield hints about self-regulating processes. Furthermore, it would be interesting to analyze quantitatively the total number of cells in the course of the GC reaction. Finally, it may be interesting to compare our model with its continuous counterpart. The translation of Eq. (3) into continuous space leads to a differential equation of Schrödinger type with a Gaussian potential.

References

- AGARWAL, A., NAYAK, B.P. & RAO, K.V.S. (1998). B-Cell Responses to a Peptide Epitope – VII – Antigen-Dependent Modulation of the Germinal Center Reaction, *J. Immunol.* **161**, 5832–5841.
- BEREK, C. & MILSTEIN, C. (1987). Mutation drift and repertoire shift in the maturation of the immune response, *Immunol. Rev.* **96**, 23–41.
- BEREK, C. & MILSTEIN, C. (1988). The Dynamic Nature of the Antibody Repertoire, *Immunol. Rev.* **105**, 5–26.
- CAMACHO, S.A., KOSCOVILBOIS, M.H. & BEREK, C. (1998). The Dynamic Structure of the Germinal Center, *Immunol. Today* **19**, 511–514.
- CASCALHO, M., MA, A., LEE, S., MASAT, L. & WABL, M. (1996). A Quasi-Monoclonal Mouse, *Science* **272**, 1649–1652.
- CHOE, J. & CHOI, Y.S. (1998). IL-10 Interrupts Memory B-Cell Expansion in the Germinal Center by Inducing Differentiation into Plasma-Cells, *Eur. J. Immunol.* **28**, 508–515.
- COHEN, J.J., DUKE, R.C., FADOK, V.A. & SELLINS, K.S. (1992). Apoptosis and programmed cell death in immunity, *Annu. Rev. Immunol.* **10**, 267–293.
- DUBOIS, B., BARTHÉLÉMY, C., DURAND, I., LIU, Y.-J., CAUX, C. & BRIÈRE, F. (1999). Toward a Role of Dendritic Cells in the Germinal Center Reaction – Triggering of B-Cell Proliferation and Isotype Switching, *J. Immunol.* **162**, 3428–3436.
- EIJK, M. VAN & GROOT, C. DE, (1999). Germinal Center B-Cell Apoptosis Requires Both Caspase and Cathepsin Activity, *J. Immunol.* **163**, 2478–2482.
- FISCHER, M.B., GOERG, S., SHEN, L.M., PRODEUS, A.P., GOODNOW, C.C., KELSOE, G. & CARROLL, M.C. (1998). Dependence of Germinal Center B-Cells on Expression of Cd21/Cd35 for Survival, *Science* **280**, 582–585.
- FLIEDNER, T.M. (1967). On the origin of tingible bodies in germinal centers in immune responses, in: H. Cottier (Hrsg.), *Germinal Centers in Immune Responses*. Springer, Berlin, pp. 218–224.
- GROUARD, G., DE BOUTELLER, O., BANCHEREAU, J. & LIU, Y.-J. (1995). Human follicular dendritic cells enhance cytokine-dependent growth and differentiation of CD40-activated B cells, *J. Immunol.* **155**, 3345–3352.
- HAN, S.H., HATHCOCK, K., ZHENG, B., KELPER, T.B., HODES, R. & KELSOE, G. (1995a). Cellular Interaction in Germinal Centers: Roles of CD40-Ligand and B7-1 and B7-2 in Established Germinal Centers, *J. Immunol.* **155**, 556–567.
- HAN, S.H., ZHENG, B., DAL PORTO, J. & KELSOE, G. (1995b). In situ Studies of the Primary Immune Response to (4-Hydroxy-3-Nitrophenyl) Acetyl IV. Affinity-Dependent, Antigen-Driven B-Cell Apoptosis in Germinal Centers as a Mechanism for Maintaining Self-Tolerance, *J. Exp. Med.* **182**, 1635–1644.
- HANNA, M.G. (1964). An autoradiographic study of the germinal center in spleen white pulp during early intervals of the immune response, *Lab. Invest.* **13**, 95–104.
- HARDIE, D.L., JOHNSON, G.D. & MACLENNAN, I.C.M. (1993). Quantitative analysis of molecules which distinguish functional compartments in germinal centers, *Eur. J. Immunol.* **23**, 997–1004.
- JACOB, J., KASSIR, R. & KELSOE, G. (1991). In situ studies of the primary immune

- response to (4-hydroxy-3-nitrophenyl)acetyl. I. The architecture and dynamics of responding cell populations, *J. Exp. Med.* **173**, 1165–1175.
- JACOB, J., PRZYLEPA, J., MILLER, C. & KELSOE, G. (1993). In situ studies of the primary response to (4-hydroxy-3-nitrophenyl)acetyl. III. The kinetics of V region mutation and selection in germinal center B cells, *J. Exp. Med.* **178**, 1293–1307.
- JANEWAY, C.A. & TRAVERS, P. (1997). Immunologie. Spektrum Akademischer Verlag, Heidelberg, Berlin, Oxford.
- KELSOE, G. (1996). The germinal center: a crucible for lymphocyte selection, *Semin. Immunol.* **8**, 179–184.
- KEPLER, T.B. & PERELSON, A.S. (1993). Cyclic re-entry of germinal center B cells and the efficiency of affinity maturation, *Immunol. Today* **14**, 412–415.
- KESMIR, C. & BOER, R.J. DE, (1999). A Mathematical Model on Germinal Center Kinetics and Termination, *J. Immunol.* **163**, 2463–2469.
- KROESE, F.G., WUBBENA, A.S., SEIJEN, H.G. & NIEUWENHUIS, P. (1987). Germinal centers develop oligoclonally, *Eur. J. Immunol.* **17**, 1069–1072.
- KÜPPERS, R., ZHAO, M., HANSMANN, M.L. & RAJEWSKY, K. (1993). Tracing B Cell Development in Human Germinal Centers by Molecular Analysis of Single Cells Picked from Histological Sections, *EMBO J.* **12**, 4955–4967.
- LINDHOUT, E., LAKEMAN, A. & GROOT, C. DE, (1995). Follicular dendritic cells inhibit apoptosis in human B lymphocytes by rapid and irreversible blockade of preexisting endonuclease, *J. Exp. Med.* **181**, (1985–1995).
- LINDHOUT, E., MEVISSSEN, M.L., KWEKKEBOOM, J., TAGER, J.M. & GROOT, C. DE, (1993). Direct evidence that human follicular dendritic cells (FDC) rescue germinal centre B cells from death by apoptosis, *Clin. Exp. Immunol.* **91**, 330–336.
- LINDHOUT, E., KOOPMAN, G., PALS, S.T. & GROOT, C. DE, (1997). Triple check for antigen specificity of B cells during germinal centre reactions, *Immunol. Today* **18**, 573–576.
- LIU, Y.-J., BARTHÉLÉMY, C., DE BOUTEILLER, O. & BANCHEREAU, J. (1994). The differences in survival and phenotype between centroblasts and centrocytes, *Adv. Exp. Med. Biol.* **355**, 213–218.
- LIU, Y.-J., JOSHUA, D.E., WILLIAMS, G.T., SMITH, C.A., GORDON, J. & MACLENNAN, I.C. (1989). Mechanism of antigen-driven selection in germinal centres, *Nature* **342**, 929–931.
- LIU, Y.-J., ZHANG, J., LANE, P.J., CHAN, E.Y. & MACLENNAN, I.C.M. (1991). Sites of specific B cell activation in primary and secondary responses to T cell-dependent and T cell-independent antigens, *Eur. J. Immunol.* **21**, 2951–2962.
- MACLENNAN, I.C.M. (1994). Germinal Centers, *Annu. Rev. Immunol.* **12**, 117–139.
- MCHEYZER-WILLIAMS, M.G., MCLEAN, M.J., LABOR, P.A. & NOSSAL, G.V.J. (1993). Antigen-driven B cell differentiation in vivo, *J. Exp. Med.* **178**, 295–307.
- NOSSAL, G. (1991). The molecular and cellular basis of affinity maturation in the antibody response, *Cell* **68**, 1–2.
- OPREA, M. & PERELSON, A.S. (1996). Exploring the Mechanism of Primary Antibody Responses to T-Cell-Dependent Antigen, *J. Theor. Biol.* **181**, 215–236.
- OPREA, M. & PERELSON, A.S. (1997). Somatic mutation leads to efficient affinity

- maturation when centrocytes recycle back to centroblasts, *J. Immunol.* **158**, 5155–5162.
- OPREA, M., NIMWEGEN, E. VAN & PERELSON, A.S. (2000). Dynamics of One-pass Germinal Center Models: Implications for Affinity Maturation, *Bull. Math. Biol.* **62**, 121–153.
- PASCUAL, V., CHA, S., GERSHWIN, M.E., CAPRA, J.D. & LEUNG, P.S.C. (1994a). Nucleotide Sequence Analysis of Natural and Combinatorial Anti-PDC-E2 Antibodies in Patients with Primary Biliary Cirrhosis, *J. Immunol.* **152**, 2577–2585.
- PASCUAL, V., LIU, Y.-J., MAGALSKI, A., DE BOUTELLER, O., BANCHEREAU, J. & CAPRA, J.D. (1994b). Analysis of somatic mutation in five B cell subsets of human tonsil, *J. Exp. Med.* **180**, 329–339.
- PERELSON, A.S. & OSTER, G.F. (1979). Theoretical Studies of Clonal Selection: Minimal Antibody Repertoire Size and Reliability of Self-Non-self Discrimination, *J. Theor. Biol.* **81**, 645–670.
- PERELSON, A.S. & WIEGEL, F.W. (1999). Some Design Principles for Immune System Recognition, *Complexity* **4**, 29–37.
- RADMACHER, M.D., KELSOE, G. & KEPLER, T.B. (1998). Predicted and Inferred Waiting-Times for Key Mutations in the Germinal Center Reaction – Evidence for Stochasticity in Selection, *Immunol. Cell Biol.* **76**, 373–381.
- RUNDELL, A., DECARLO, R., HOGENESCH, H. & DOERSCHUK, P. (1998). The Humoral Immune-Response to Haemophilus-Influenzae Type-B – A Mathematical-Model Based on T-Zone and Germinal Center B-Cell Dynamics, *J. Theor. Biol.* **194**, 341–381.
- SMITH, K., LIGHT, A., NOSSAL, G. & TARLINGTON, D. (1997). The extent of affinity maturation differs between the memory and antibody-forming cell compartments in the primary immune response, *EMBO J.* **16**, 2996–3006.
- TEW, J. & MANDEL, T. (1979). Prolonged antigen half-life in the lymphoid follicles of specifically immunized mice, *Immunology* **37**, 69–76.
- DE VINUESA, C.G., COOK, M.C., BALL, J., DREW, M., SUNNERS, Y., CASCALHO, M., WABL, M., KLAUS, G.G.B. & MACLENNAN, C.M. (2000). Germinal Centers without T Cells, *J. Exp. Med.* **191**, 485–493.
- WEDEMAYER, G.J., PATTEN, P.A., WANG, L.H., SCHULTZ, P.G. & STEVENS, R.C. (1997). Structural insights into the evolution of an antibody combining site, *Science* **276**, 1665–1669.
- WEIGERT, M., CESARI, I., YONKOVITCH, S. & COHN, M. (1970). Variability in the light chain sequences of mouse antibody, *Nature* **228**, 1045–1047.
- ZHANG, J., MACLENNAN, I.C.M., LIU, Y.-J. & LAND, P.J.L. (1988). Is rapid proliferation in B centroblasts linked to somatic mutation in memory B cell clones, *Immunol. Lett.* **18**, 297–299.